PHILOSOPHICAL TRANSACTIONS OF THE ROYAL SOCIETY A MATHEMATICAL, PHYSICAL & ENGINEERING SCIENCES

First Neutral-Beam Heating Experiments in JET

G. Duesing, P. Lomas, A. Stabler, P. Thomas and E. Thompson

Phil. Trans. R. Soc. Lond. A 1987 **322**, 109-123
doi: 10.1098/rsta.1987.0041

Phil. Trans. R. Soc. Lond. A **322**, 109–123 (1987)
Printed in Great Britain

First neutral-beam heating experiments in JET

By G. Duesing, P. Lomas, A. Stäbler, P. Thomas and E. Thompson
*JET Joint Undertaking, Abingdon, Oxfordshire OX*14 3*EA U.K.*

Hydrogen beams at particle energies of up to 65 keV, total beam powers of up to 5.5 MW, and beam-pulse durations of up to 7 s have been injected into deuterium plasmas. Experiments were performed over a wide range of plasma parameters with limiter plasmas and inner-wall plasmas. The operational régime was extended by 70% over the current ohmic density limit. In medium density experiments, ion temperatures of *ca.* 6.5 keV were reached with electron temperatures of 4.8 keV. The expected degradation of energy confinement with additional heating was observed. At 4 MA plasma current and 8 MW total input power, the global energy confinement time is *ca.* 0.4 s. The metallic impurity concentration and Z_{eff} drop with the rise of plasma density during beam pulses. The rise of radiated power closely follows that of the density. In most cases, the highest value of the radiated power stays below 50% of the power input, with very low radiation from the centre of the plasma.

1. Introduction

The heating of tokamak plasmas by powerful beams of energetic hydrogen or deuterium atoms is based on the formation and electrostatic acceleration of beams of positive ions, which then have to be converted to neutral atoms in order to enable their passage through the tokamak field. At the high particle energies of 60–80 keV per atomic mass unit required for particle deposition close to the plasma axis, the neutralization technique that was used, namely firing the beams through hydrogen gas cells, has an efficiency of only *ca.* 45–24%. The non-neutralized beam fractions are magnetically deflected and dumped in the beam-line system. When penetrating the plasma, the fast atoms become ionized mainly by impact ionization and charge exchange with the plasma hydrogenic ions and to a lesser extent by charge exchange with impurity ions, with a small contribution from ionization by the electrons. Consequently, the fast ions are trapped within the plasma, and then dissipate their kinetic energy by Coulomb scattering with the plasma ions and electrons. This well-proven technique and the underlying physics have been summarized on various occasions (see, for example, Sweetman *et al.* 1981).

The main new feature of the JET neutral-beam injectors is their design for long (*ca.* 10 s) beam-pulse operation. JET will have two injectors comprising eight beam sources each. Initially, the injectors will be operated at particle energy of 80 keV or less with hydrogen or deuterium. With hydrogen operation at 80 keV the extracted ion-beam power from each source is 4.8 MW. Operation with the first injector has started, the second will come into operation in 1987. In 1988 and 1989, respectively, the two injectors will be modified for deuterium operation at 160 keV or less.

This paper reports on the first month of JET experiments with neutral-beam heating, during which hydrogen from eight beam sources was injected into deuterium plasmas, with beam-particle energies (in the full energy fraction) in the range of 45–65 keV. After a short description of the injector and a summary of computations on particle and heating power

deposition in the plasma in §2, several individual heating experiments, performed by firing the beams into different types of plasmas, will be described in §3, and parameter scans on plasma current and beam power, which were performed to investigate the density limit and the energy confinement, in §4.

At the time of writing the paper, only a preliminary evaluation of the experiments had been carried out. In particular, most of the diagnostic data and the given levels of beam power into the plasma should be considered as provisional.

During all experiments reported here, the tokamak was operated with eight small graphite limiters (total surface area *ca.* 2.4 m^2) on the outer wall of the vacuum vessel ('torus') and the inner wall was completely covered with graphite protection tiles. The Inconel torus wall had been carbonized at an earlier time and was kept at 300 °C during operation.

2. Injection system

The first neutral injector has been described elsewhere (Duesing 1984). The multibeamlet beams have a cross section of 45 cm × 18 cm at the source, a species mix for 80 kV operation of $H^+:H_2^+:H_3^+ = 85\%:11\%:4\%$ at 60 A (and $D^+:D_2^+:D_3^+ = 82\%:11\%:7\%$ at 42 A) perveance-matched current, and a beamlet divergence of 0.7° for the hydrogen species (and 0.5° for the deuterium species). The impurity level in the beams in total is below a limit of detectability of 1%; the level of light impurities, particularly oxygen, is less than 0.5%, as determined by H_α doppler shift spectroscopy (Hemsworth 1986). The eight beam sources are arranged in two vertical groups of four. The injection geometry for the two groups of beams is shown in figure 1. The more normal beams cross the torus once and are intercepted by its

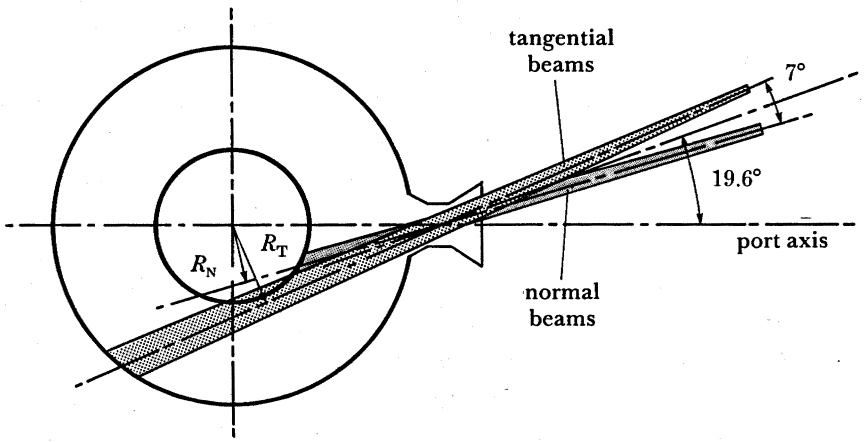

Figure 1. Plan view of the injection geometry. $R_N = 1.31$ m, $R_T = 1.85$ m.

inner wall, which in the individual areas of beam impact, is monitored by infrared diodes forming one branch of the beam-plasma interlock system. The more tangential beams cross the torus twice, almost touching the inner wall. The radii of tangency to the plasma are $R_N = 1.31$ m for the 'normal' and $R_T = 1.85$ m for the 'tangential' beams.

The integrated beam-line system (Haange *et al.* 1986) for the eight beams, in addition to handling the non-neutralized beam fractions, also has the function of scraping the beam edges

for the entrance through the torus port, and close to its exit includes a retractable calorimeter to determine the power density profiles and positions of the beams through the full pulse duration. The gas pressure downstream of the ion deflection magnet is kept at *ca.* 5×10^{-5} mbar† by means of a cryopump with 8×10^6 l s^{-1} hydrogen-pumping speed (Obert *et al.* 1984), in order to limit the re-ionization. The beam-line system including a simulation of the torus duct scrapers has been tested (Falter *et al.* 1986) and the power distribution determined in the JET test bed. This test did not include a simulation of the re-ionization nor of the tokamak magnetic field.

The beam power transferred into the torus is evaluated from the power into the calorimeter and, with the calorimeter retracted, the water calorimetric determination of the power into scrapers on the calorimeter rear side, injector box exit scrapers, inner liners of the vacuum valve between injector box and torus, and torus duct scrapers. The power levels given throughout this paper are these powers into the torus. To deduce heating powers to the plasma, corrections for charge-exchange losses from the fast ions, orbit losses and beam shine-through have to be made, which together are estimated to amount normally to a few percent each, but have not yet been incorporated in the results of figures 12 and 13.

Computations have been performed (Watkins & Stubberfield 1986) of the fast-ion generation rate and the power deposition density in the plasma, by using measured density and electron temperature profiles. The results are presented in figure 2 for the 65 keV (full energy component) hydrogen injection into deuterium and for the plasma of JET pulse no. 7155 (see

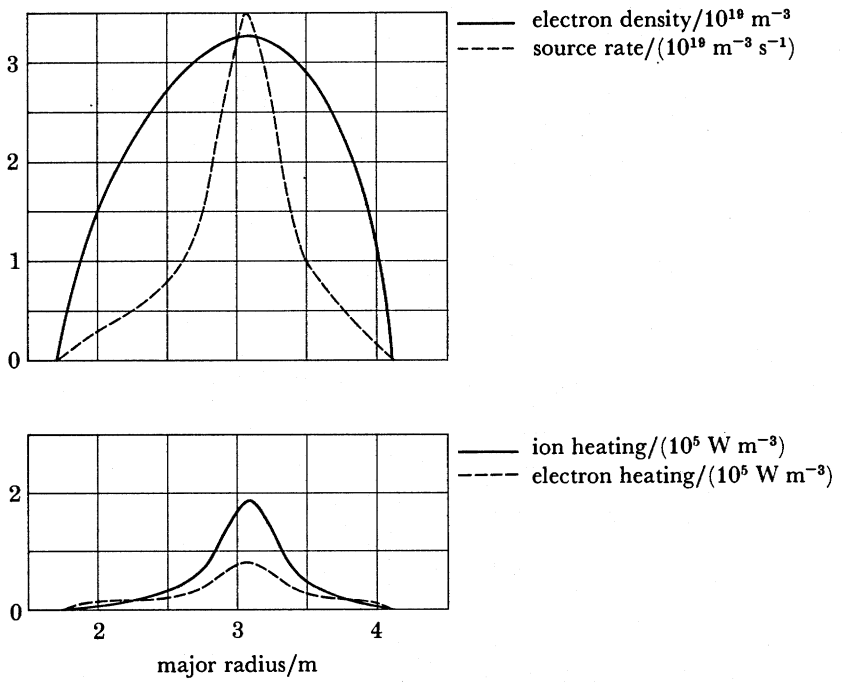

FIGURE 2. Beam-power deposition profiles computed (Watkins & Stubberfield 1986) for pulse no. 7155 at 10 s. $H^0 \rightarrow D^+$ injection at 65 keV (main energy component) and 5.5 MW total power. The top part shows the electron density as measured, and the fast-ion generation rate. The bottom part shows power densities for the ion and electron heating.

† 1 bar = 10^5 Pa.

§3) at 10 s, when the plasma density was $\bar{n}_e = 2.3 \times 10^{19}$ m^{-3}. The total power from the eight beams was 5.5 MW, the power fractions were 69, 23 and 8% in the full, half and third energy components, respectively. With the electron temperature being $T_e^0 \approx 5$ keV at the chosen time, 2.2 MW were coupled to the electrons and 3.1 MW to the ions. The shine-through fraction (all from the normal beams) was calculated to be 3% of the total power. The figure shows the profiles of the fast-ion generation rate, and the electron and ion heating power densities. There is little difference in the profiles from the individual beams, the figure shows their superposition. The profiles are peaked on axis, which was also found, though less pronounced, for the highest densities achieved so far, namely $\bar{n}_e = 5.2 \times 10^{19}$ m^{-3}.

3. Inidividual heating experiments

3.1. *High-density plasma*

Stable plasma operation at high densities was achieved for a variety of parameter values. As an example, this section describes a pulse (no. 7145) where beams at $P_b = 5.5$ MW were injected into a 4 MA plasma (figure 3). The plasma leans on the limiters, but is terminated

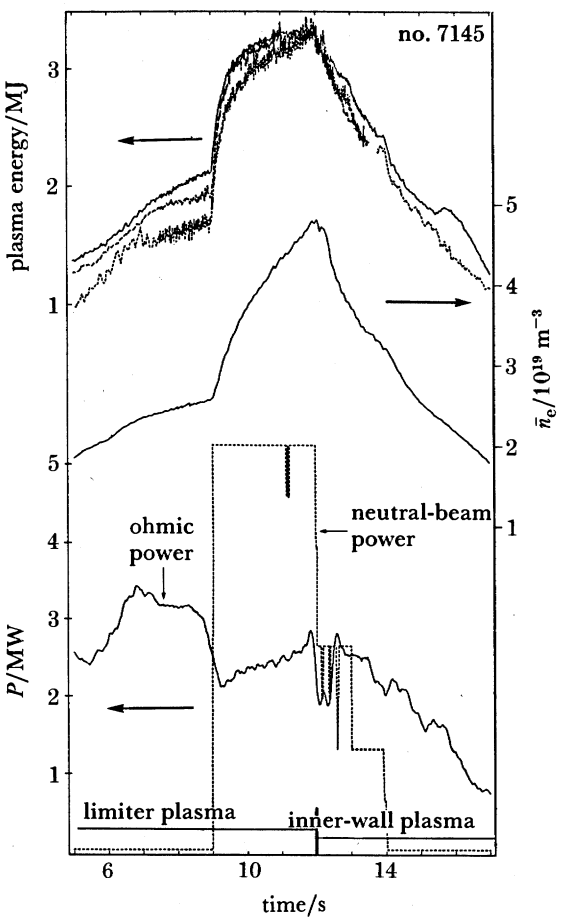

Figure 3. Neutral-beam power, ohmic power, line-averaged electron density $\bar{n}_e$, and plasma stored energy (from three different measurements) in a 4 MA limiter plasma, that is terminated on the inner wall. Plasma current flat top from 7 to 12 s.

by shifting it to the inner wall. This recipe (used in JET before) was found to be useful; the inner wall apparently is able to pump the high density built up by the beams. The beam switch off is staggered. The ohmic power, P_{OH}, drops by *ca.* 1 MW at beam switch on. (The apparent slow P_{OH} drop and certain P_{OH} overshoots in the graph are due to the applied automatic smoothing of the measured signals.) The drop in ohmic power reflects the loop voltage drop, which is due to a combination of beam-driven current, electron heating and fall in the measured effective ionic charge, Z_{eff}.

The figure also shows the steep increase of the line-averaged electron density, $\bar{n}_e(t)$, with the beam onset, and the smooth density decay after the plasma is moved to the inner wall. By injecting the neutral beams, the density range accessible has been extended by *ca.* 70% above the ohmic limits observed in present JET operation. The density ramp rate was found to be larger than the beam-particle source rate initially, and comparable with that rate later in the pulse during the further, nearly linear rise.

Figure 3 further shows the increase in total plasma stored energy, $W(t)$, due to beam injection, from kinetic, diamagnetic and magnetic equilibrium measurements. The stored plasma energy is doubled and reaches the value of 3.3 MJ.

The ion temperature, as determined by four different methods (Sadler *et al.* 1986; von Hellermann *et al.* 1986), is shown in figure 4. Whereas there is some spread in the absolute value of the ion temperature, all four methods show an increase of *ca.* 1 keV at the beginning of the beam pulse, which is largely maintained during its duration. The electron temperature goes up from 3.8 to 4.8 keV when the beams are switched on. As the density builds up, the electron temperature gradually decreases to 3.4 keV at the end of the full-power beam pulse.

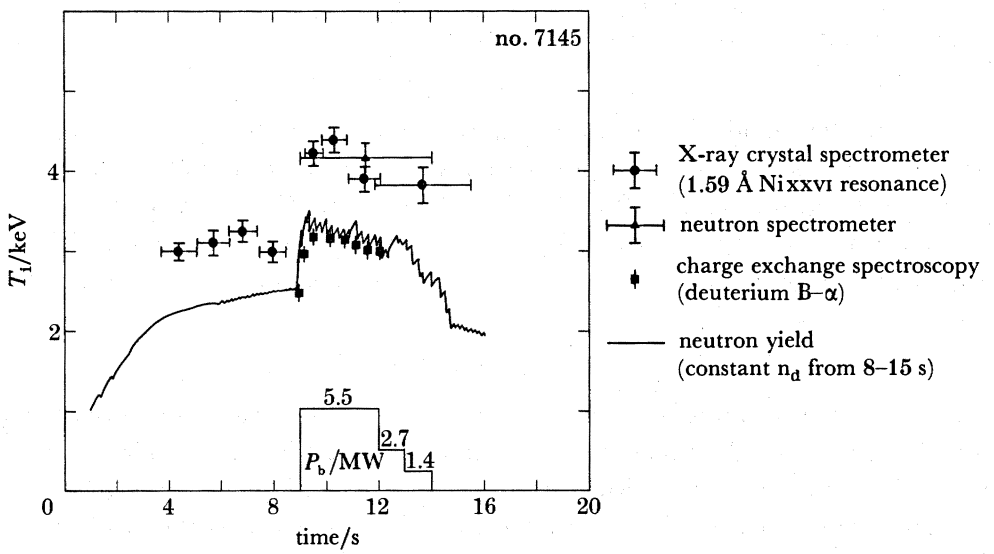

FIGURE 4. Ion temperature from four diagnostics for the high-density plasma at 4 MA and 3.4 T, shown in figure 3.

The radiated power evolution $P_{rad}(t)$ (Jäckel *et al.* 1986) closely follows the density rise indicating that the impurity density stays approximately constant during the increase in plasma density. It reaches its maximum at the end of the beam pulse with a value equivalent to 43% of the total power input, $P_{tot} = P_{OH} + P_b$. The radiation chordal profiles (figure 5) show a low

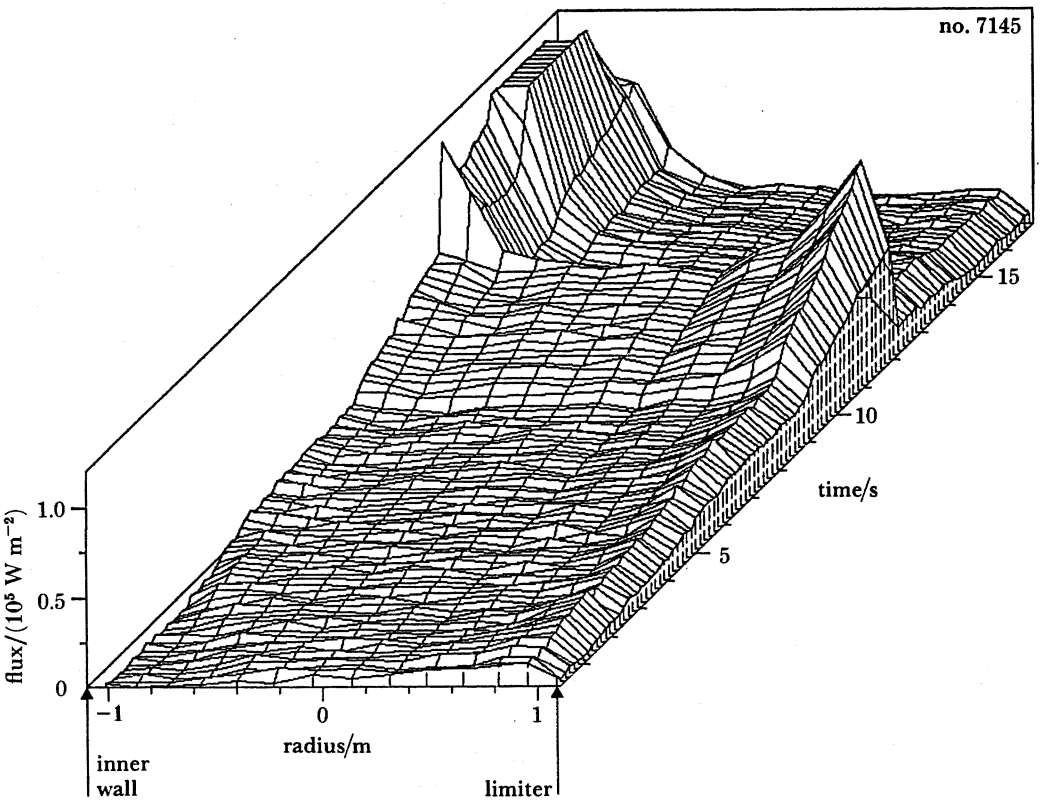

FIGURE 5. Radiated power profile (Jäckel *et al.* 1986) from a vertical bolometer array (not Abel inverted) for the plasma shown in figure 3, with 5.5 MW neutral beams starting at 9 s. The flux is normalized to radiation into 4π solid angle. At 12 s the plasma is moved to the inner wall.

central radiation all through the pulse. Z_{eff} as measured by the visible bremsstrahlung decreases from 3.2 to 2.6. The spectroscopic impurity survey during the beam pulse gives a result very similar to that found during high density ohmic discharges. However, oxygen becomes the dominant impurity, whereas the carbon concentration (dominant in the ohmic part of the discharge) drops substantially, as does the concentration of nickel, the strongest metallic impurity.

3.2. *Inner-wall plasmas*

The above-mentioned pumping effect exhibited by the inner wall of the torus occurs when the plasma is moved inwards so that the inner wall rather than the limiters define the outermost flux surface. In the discharges described in this section, the plasma was moved to the inner wall during the early part of a beam pulse in an attempt to obtain essentially steady-state plasma conditions during the application of beams.

The typical behaviour of such discharges is shown in figure 6. In this example (no. 6984), injection of 4.4 MW into the 3 MA target plasma with $B_{\text{T}} = 2.8$ T was initiated at 8 s, and the plasma was detached from the limiter and moved into contact with the inner wall at 9 s. The rapid increase of plasma density appropriate to injection into the limiter discharge is strongly reduced during the subsequent 4 s of injection with the plasma limited by the inner wall. The volume averaged density increases by *ca.* 15 % during this time. The higher derivative of the axial density indicates some peaking of the density profile.

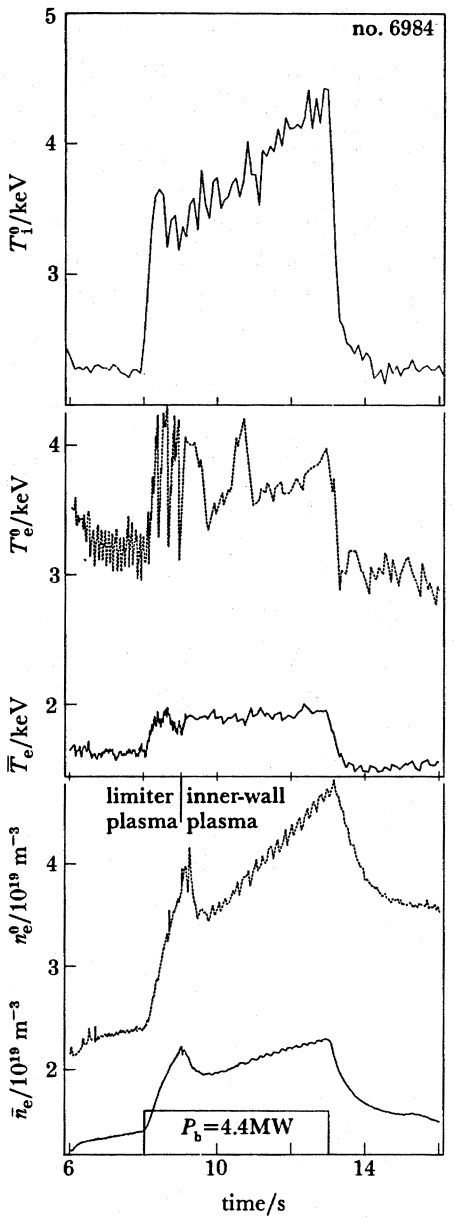

FIGURE 6. Beam injection at 4.4 MW into a 3 MA plasma that is moved to the inner wall 1 s after beam initiation. The time evolution is shown of the volume averaged and the axial density, the volume averaged and the axial electron temperature, and the ion temperature from the central channel of a neutral particle analyser. The axial electron temperature is distorted by the slow sampling rate after 9 s, which cannot cover the *ca.* 1 keV sawteeth.

The volume averaged electron temperature during beam injection remains constant as apparently does the axial value. The figure also shows the ion temperature from the central channel of the neutral-particle analyser. This measurement is in reasonable agreement with the ion-temperature evolution from the width of a Ni XXVI line.

It is a characteristic of this type of operation that the radiated power is approximately equal to the level of the ohmic input only, which would suggest that power at the level of the neutral beam power is lost essentially via conduction and convection processes.

3.3. *High-ion-temperature plasmas*

It has been observed in tokamaks with intense additional heating that the plasma energy content is essentially independent of the electron density (Kaye 1985 and references therein). Consequently the highest temperatures should be expected at low density. Furthermore, at low density and high electron temperature, the energy transfer between the beam and plasma ions is maximized whereas the importance of equipartition with the electrons is reduced. This is the so called 'hot-ion régime' which has been used in PLT (Goldston *et al.* 1980) and other machines to demonstrate ion temperatures in the 7–8 keV range.

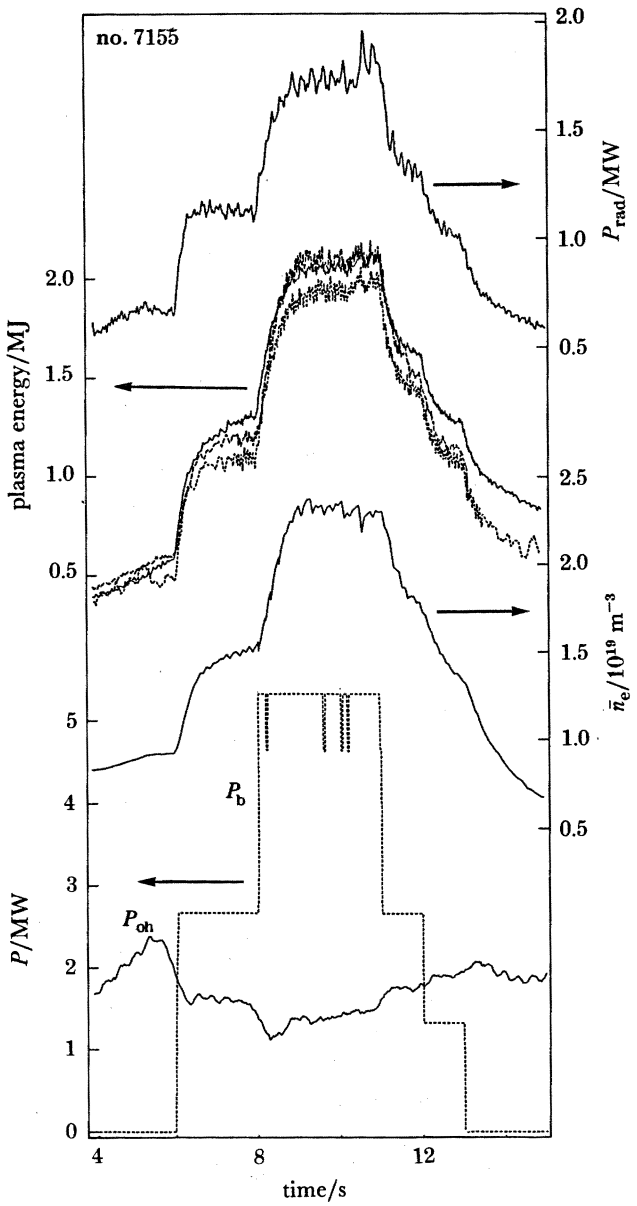

FIGURE 7. Neutral-beam power P_b, ohmic power P_{OH}, line-averaged electron density $\bar{n}_e$, plasma stored energy, and total radiated power P_{rad} (from bolometer measurements) in a 3 MA plasma (flat top from 5 to 15 s) limited by the inner wall.

In order to operate JET in the 'hot-ion régime' the plasma must be pumped by the inner wall, as described in §3.2. It was found that moving the plasma to the inner wall during the current rise was sufficient to ensure both a low target density and a minimal density rise during neutral beam injection. A selection of diagnostic traces for a pulse of this type is shown in figures 7 and 8. Pulse no. 7155 had a flat-top current of 3 MA and a toroidal field of 2.8 T. The plasma

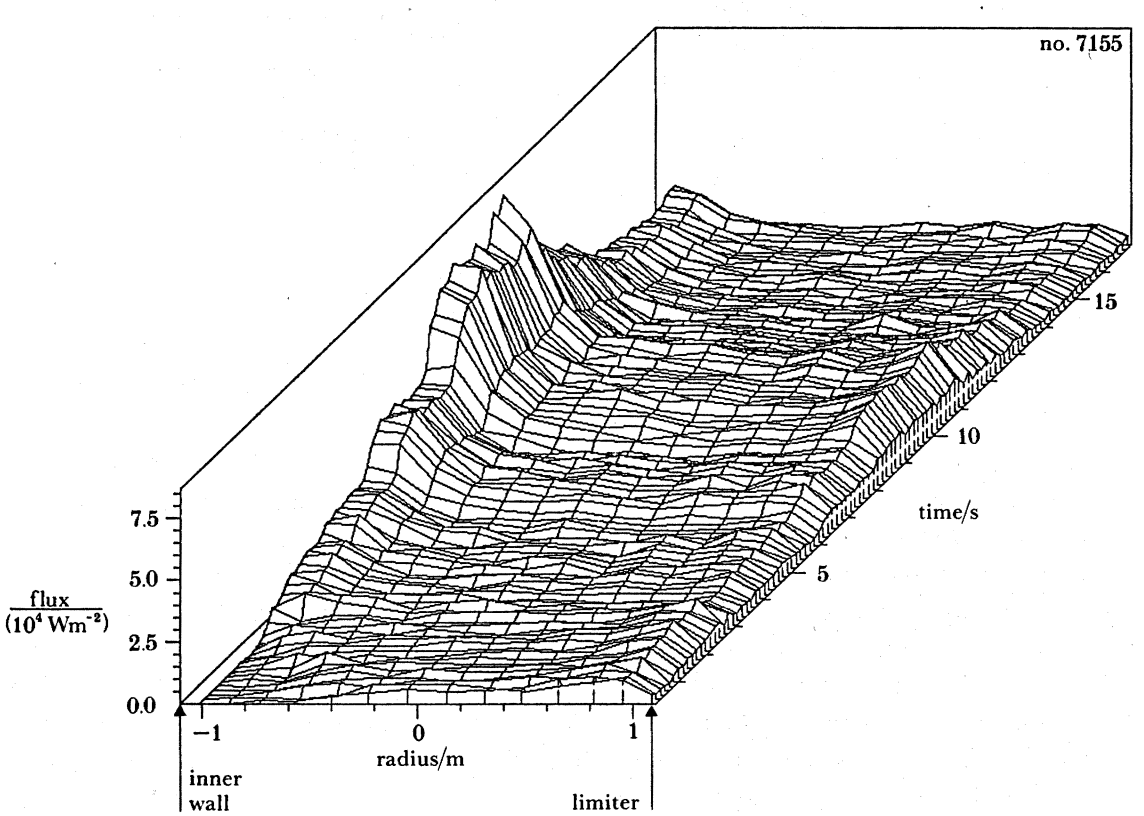

FIGURE 8. Radiated power profile (Jäckel *et al.* 1986) from a vertical bolometer array (not Abel-inverted) for the plasma shown in figure 7, neutral beams starting at 6 and 8 s.

moved to the inside wall at 3 s and the current flat top lasted from 5 to 15 s. The neutral beam power was stepped up to reach 5.5 MW between 8 and 11 s. During the heating pulse the ohmic input dropped from 2.4 MW to around 1.5 MW. The line-averaged electron density climbed from 0.9 to 2.3×10^{19} m^{-3}. The maximum central density was 3.1×10^{19} m^{-3}. The power radiated from the plasma during the beam pulse was 1.7 MW or about 25% of the total input. The central electron temperature rose from 4.1 to 4.8 keV at maximum power.

Four different estimates of the ion temperature are presented in figure 9. It must be stressed that they all require corrections that have not as yet been applied. The X-ray crystal spectrometer measures the Doppler broadening of the 1.59 Å Ni XXVI resonance line†. In addition to some instrumental effects, this measurement has not been corrected for the temperature averaging which occurs because the emission volume is finite. The crystal spectrometer is aligned so that it can detect plasma rotation in the toroidal direction. The beam

† 1 Å = 10^{-1} nm = 10^{-10} m.

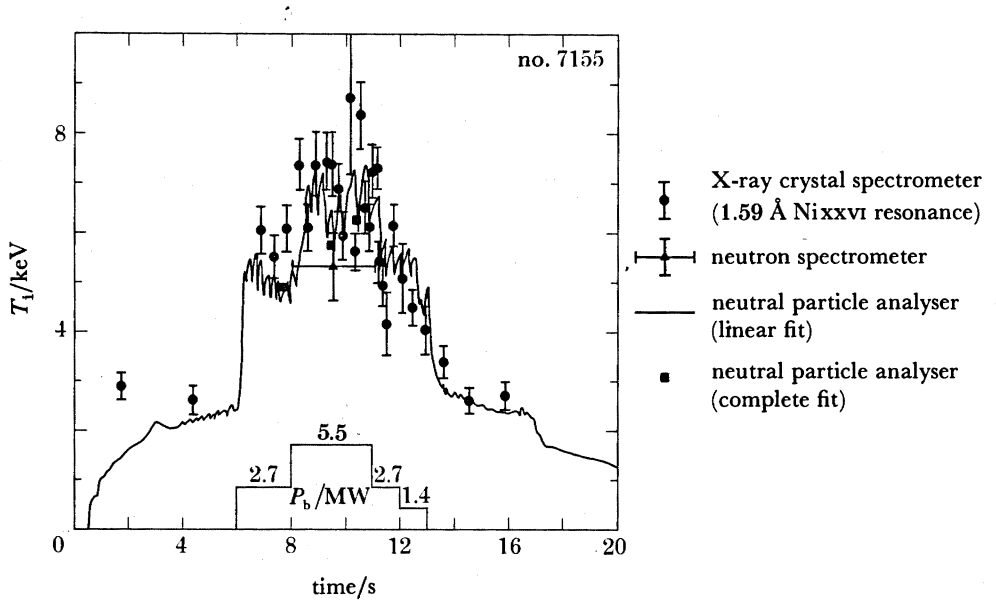

FIGURE 9. Ion temperature from three diagnostics for the low density, 3 MA, 2.8 T plasma shown in figure 7.

momentum imparted a peak velocity of 1.6×10^5 m s^{-1} to the plasma in this pulse. The implications of this measurement have not yet been determined. The neutron spectrometer measures the Doppler broadening of the 2.45 MeV d–d neutron peak. This also requires correction for the averaging over the emission volume. It is estimated that the peak deuteron temperature is approximately 8% greater than that shown. The data from the neutral particle analyser have been analysed in two different ways. The solid curve in figure 9 is the temperature derived from the energy spectrum of neutral deuteron emission in the range 2 T_i to 40 keV seen by a detector, which views the plasma centre. This estimate relies on the assumption that the tail of the neutral distribution emanates from the plasma centre. In high-density pulses, such as that described in §3.1, this assumption is not justified because the plasma is nearly opaque to neutrals emitted from the centre. The neutral particle analyser points result from a determination of the deuteron temperature profile which uses data from four of the neutral particle analysers, computations of the neutral hydrogen distribution and of the plasma opacity. Taken together these data show that in this pulse the deuteron temperature rose from 2.2 to approximately 6.5 keV when 5.5 MW of neutral-beam heating was applied.

4. PARAMETER SCANS

4.1. *Operational régime*

Figure 10 shows the Hugill diagram where data have been plotted for confinement experiments with ohmic heating, for RF heating experiments and for neutral-beam heating experiments. For the case of neutral-beam heating, data have also been included where the discharge was on the point of disruption as indicated by a rapid increase in radiated power. Clearly the region in the Hugill diagram where reliable operation is readily achieved has been considerably expanded from $\bar{n}_e Rq/B_T \approx 10^{20}$ m^{-2} T^{-1} to $\bar{n}_e Rq/B_T \leqslant 2 \times 10^{20}$ m^{-2} T^{-1}. The disruptive density limit for the ohmic-heating target plasmas used for neutral-beam heating

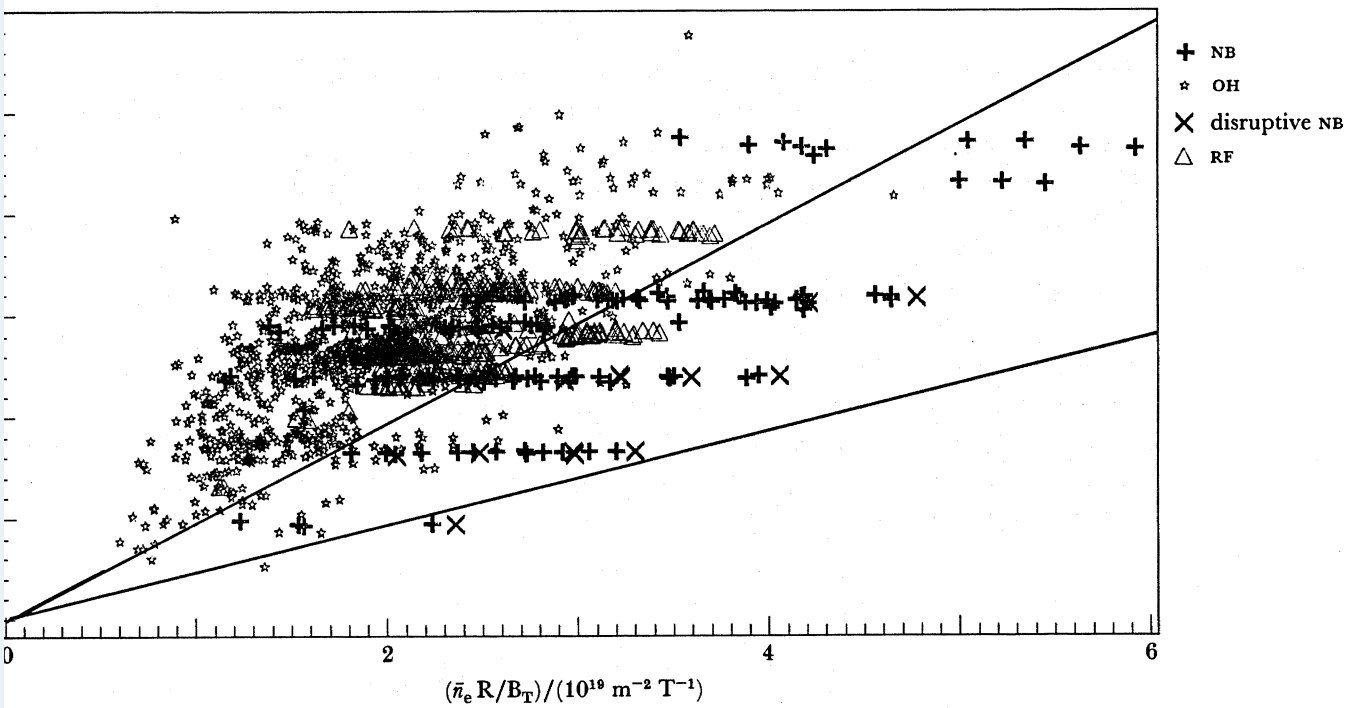

FIGURE 10. Hugill diagram for all non-disruptive JET discharges. The two slopes are for $\bar{n}_e Rq_{cyl}/B_T = 10$ and $20 \times 10^{19}\ m^{-2}\ T^{-1}$.

was in the region $\bar{n}_e Rq/B_T = 1 - 1.2 \times 10^{20}\ m^{-2}\ T^{-1}$, whereas with neutral beam heating the density at which disruption occurs increases with neutral beam power, as illustrated in figure 11, with no noticeable saturation at the highest neutral beam power. Interestingly, the highest densities reached here correspond to values of $\bar{n}_e Rq/B_T$ at which DITE (Axon *et al.* 1981) and ASDEX (Niedermayer 1985) report a weaker than linear dependence on beam power, and are comparable to the disruptive density found on Doublet III (1984) and FT (Alladio *et al.* 1983). On JET, disruptions have occurred at values of $\bar{n}_e Rq/B_T \approx 2 \times 10^{20}\ m^{-2}\ T^{-1}$ even in ohmic discharges, particularly at high q during the late current decay, but there is no evidence that this is in any sense a hard disruptive limit.

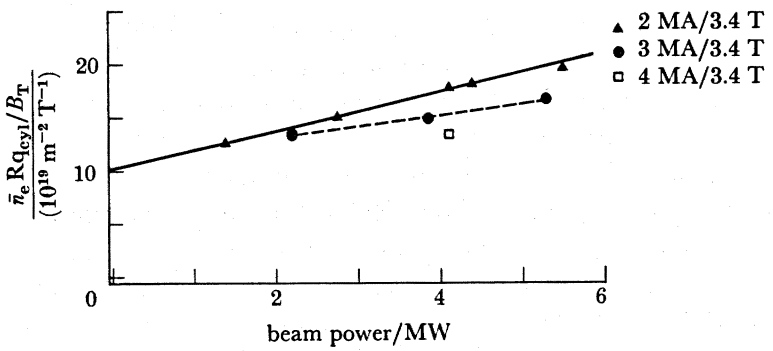

FIGURE 11. Predisruptive neutral beam heated discharges at various plasma currents. No saturation of the density limit with increasing beam power is noticeable so far.

4.2. *Confinement*

First systematic studies of the confinement behaviour of neutral-beam-heated plasmas in JET were done by varying the plasma current from 1.0 to 4.0 MA at $B_T = 3.4$ T in steps of 1.0 MA (corresponding q_{cyl} variation: 3.1–10.5). At each parameter variation, shots with different beam powers (i.e. different number of beam sources at unchanged beam energy) were carried out. The plasma ($R = 2.97$ m, $a = 1.2$ m, $b/a = 1.45$) was kept at the outside limiters during the neutral-beam pulse of up to 5 s pulse length and then moved to the inner wall to avoid high-density disruptions. As mentioned above, the plasma density increases during neutral injection. Owing to the different beam fuelling rates at different power levels and to the power-dependent density limit, the plasma densities at which the stored plasma energy approached its equilibrium values also vary, e.g. for 4.0 MA and two beams this density was $\bar{n}_e = 3.7 \times 10^{19}$ m^{-3} and for eight beams $\bar{n}_e = 4.9 \times 10^{19}$ m^{-3}. The densities were lower at lower plasma currents. All this implies that the results presented below may still contain a certain $\bar{n}_e$ dependence that is not yet worked out.

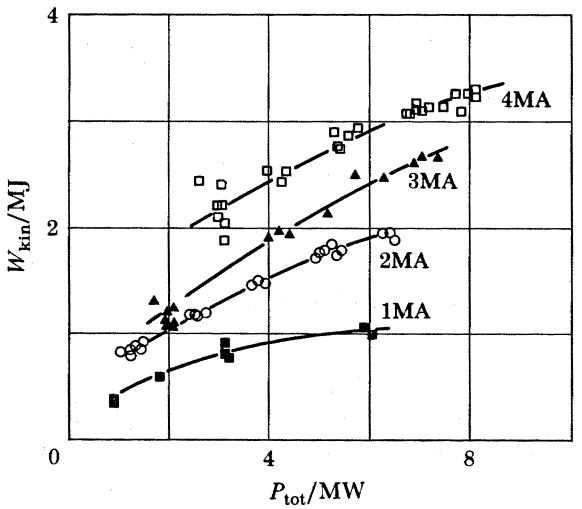

FIGURE 12. Stored energy W_{kin} from kinetic measurements as a function of total input power $P_{tot} = P_{OH} + P_b$, for beam power scans in limiter plasmas at various I_p and at 3.4 T. The experimental error in the W_{kin} values is $\pm 15\%$.

Figure 12 shows the stored plasma energy measured during the current scan experiments as a function of the total (ohmic plus beam) heating power. The stored energies given in this figure are deduced from temperature and density measurements (kinetic data) and do not, therefore, include contributions from the circulating beams and the plasma rotation. Stored energies calculated from magnetic measurements (equilibrium beta corrected for the plasma inductance) and diamagnetic beta agree reasonable well with the kinetic data at higher plasma currents (3.0 and 4.0 MA) where the deviations are less than $\pm 15\%$, whereas at the lower values of plasma current this difference increases to up to $\pm 35\%$. Presently, the kinetic data are considered to be the most reliable and are used for further analysis. The experimental error in the kinetic stored energy data amounts to $\pm 15\%$. The scatter in the data also reflects a weak density dependence.

The points in figure 12 belonging to different values of plasma current are clearly separated. The increment in stored energy over the pure ohmic values (represented by the lowest power points in the figure) with increasing beam power is not significantly dependent on the plasma current in the range 2.0–4.0 MA. The separation of the points belonging to different I_p values is therefore mainly due to the separation already present in the ohmic energy content. It should be noted that at high values of plasma current the contribution of the ohmic input power to the total heating power is still significant, e.g. at $I_p = 4$ MA: $P_b \leqslant 5.5$ MA, $P_{OH} = 2.6$–3.1 MW, so that an unambiguous investigation of the confinement scaling with plasma current in beam dominated plasmas can only be performed when higher beam powers become available.

The global energy confinement times derived from the data in figure 12 are plotted in figure 13 against total input power. Obviously, the confinement degrades with increasing additional heating power as observed in other limiter tokamaks (L-mode (Goldston 1984)). The range in additional power is still insufficient to determine whether the confinement time will continue to degrade or approach a saturation value for very high power input.

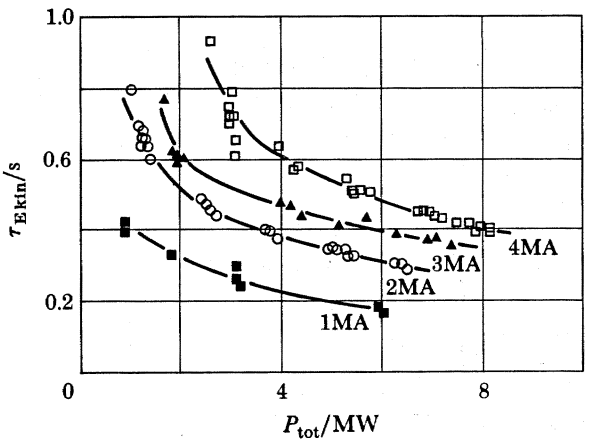

FIGURE 13. Global energy confinement time $\tau_{E,\,kin} \equiv W_{kin}/P_{tot}$ for beam power scans in limiter plasmas at various I_p and at 3.4 T.

It is interesting to note that the absolute confinement times at 3.0 MA and 4.0 MA are fairly well described by the Kaye–Goldston L-mode scaling (Kaye & Goldston 1985) derived from the results on various smaller tokamaks. This implies that the size scaling found there is proved to be valid for the step from $a \leqslant 0.45$ m, $R \leqslant 1.65$ m to JET dimensions. The I_p dependence of τ_E in the Kaye–Goldston scaling, however, is certainly stronger than found so far in the experiments reported here.

5. SUMMARY

A long-pulse neutral-beam injector with eight beam sources has been taken into operation on JET. The paper reports on the preliminary evaluation of the first month of neutral-beam heating experiments. Deuterium plasmas in the range $I_p = 1$–4 MA at 2.8 and 3.4 T, leaning on the limiters or on the inner wall, were heated with hydrogen beams at particle energies in the range 45–65 keV, at up to 5.5 MW injected beam power and up to 26 MJ injected energy per pulse.

At the beam-particle energies used, the power-density deposition profiles were peaked on axis, even for the highest plasma densities achieved so far. No dependence of plasma behaviour on the different geometries of the eight beams was observed nor expected from computations.

The operational régime was extended to line-averaged densities of $\bar{n}_e = 5.2 \times 10^{19}$ m^{-3}, and Murakami parameters $\bar{n}_e R/B_T = 5.9 \times 10^{19}$ m^{-2} T^{-1}, which are both *ca.* 70% above the present ohmic limits. Operation at $\bar{n}_e Rq_{cyl}/B_T = 20 \times 10^{19}$ m^{-2} T^{-1} was achieved, substantially better than previously published results (Bickerton *et al.* 1986).

The plasma stored energy was raised by about a factor of two. The energy confinement showed the expected degradation with additional heating. In a 4 MA plasma at $P_{tot} = 8$ MW input power, the global energy confinement time had the value $\tau_E \equiv W/P_{tot} = 0.4$ s corresponding to *ca.* 50% of the 4 MA ohmic value. The beam power levels achieved were still insufficient to decide on the possible existence of a saturation value for τ_E. At high values of P_{tot}, τ_E appeared to depend less than linearly on I_p.

Impurity production was not a problem in the neutral beam-heated discharges. The total radiated power increased nearly linearly with $n_e(t)$, and at its highest level normally amounted

TABLE 1. KEY JET STAFF DURING THE FIRST NBH EXPERIMENTS

name	function
E. Thompson J. Carwardine C. Challis R. Claesen A. P. H. Goede T. T. C. Jones W. Obert R. L. Roberts A. Stäbler D. Stork	neutral-beam operation
G. Duesing P. Lomas D. Stork P. Stott P. Thomas E. Thompson	session leaders
E. Kallne	X-ray crystal spectrometer
H. Jäckel	bolometer
S. Corti	neutral particle analyser
N. von Hellermann	active beam CX spectrometer
N. Jarvis	neutron yield
G. Sadler	neutron spectrum
E. Bertolini P. Chuilon B. Green J. How P. J. Mondino P. Noll	engineers-in-charge
M. Brusati A. Costley B. de Kock A. Gondhalekar R. Granetz M. Malacarne	physicists-in-charge

to 25–45% of the total input power in stable discharges. Radiation from the centre was very low in all cases. Z_{eff} decreased during beam pulses. Metallic impurity concentrations were already very low during the ohmic phase of the discharges and dropped substantially during beam pulses.

In 3 MA plasmas at $\bar{n}_e = 2.3 \times 10^{19}$ m^{-3}, central ion temperature increases from *ca.* 2.2 to *ca.* 6.5 keV were obtained with the central electron temperature increasing to 4.8 keV. The toroidal rotation velocity of the plasma was 1.6×10^5 m s^{-1} in these plasmas.

The reported experiments have been made possible by the high dedication of the staff of Neutral Beam Heating Division and a group in Power Supply Division who have built and commissioned the injector and its power supplies. The authors appreciate the participation of many JET staff in the running of the experiments of whom a few are listed in table 1. Part of the injector, namely the beam sources, have been jointly developed by JET, the CEA Fontenay-aux-Roses laboratory and the UKAEA Culham laboratory.

References

Alladio, F. *et al.* 1983 In *Proc. 11th European Conference on Controlled Fusion and Plasma Physics, Aachen, 5–9 September 1983* (*Europhysics conference abstracts*).

Axon, K. B. *et al.* 1981 In *Proc. 8th International Conference on Plasma Physics and Controlled Nuclear Fusion Research, Brussels, 1–10 July 1980*. Vienna: IAEA.

Bickerton, R. J. *et al.* 1986 In *Proc. 12th European Conference on Controlled Fusion and Plasma Physics, Budapest, 2–6 September 1985* (ed. G. Grieger) (*Plasma Phys. controlled Fusion* **28**, 55).

Doublet III 1984 Annual Report for period Oct. 1983–Sept. 1984, GA-A18024.

Duesing, G. 1984 In *Proc. 13th Symposium on Fusion Technology, Varese, 24–28 September 1984*, p. 59.

Falter, H. D., Hemsworth, R. S., Deschamps, G. H., Goede, A. P. H., Jones, T. T. C., Massmann, P., Mead, M. J. & Stäbler, A. 1986 In *Proc. 11th Symposium on Fusion Engineering, Austin, 18–28 November 1985* (ed. J. Evans, O. Jones & D. C. Wilkins). New York: IEEE.

Goldston, R. *et al.* 1980 In *Proc. 2nd Joint Grenoble–Varenna International Symposium, Como*, vol. 2, p. 711. Brussels: CEC.

Goldston, R. 1984 *Plasma Phys. controlled Fus.* **26**, 87.

Haange, R., Altmann, H., Papastergiou, S., Tivey, R. & Watson, M. 1986 In *Proc. 11th Symposium on Fusion Engineering, Austin, 18–22 November 1985* (ed. J. Evans, O. Jones & D. C. Wilkins). New York: IEEE.

von Hellermann, M., Engelhardt, W. W., Horton, L., Carolan, P., Forrest, M. & Peacock, N. 1986 In *Proc. 13th European Conference on Controlled Fusion and Plasma Heating, Schliersee, 14–18 April 1986* (ed. G. Briffod & M. Kaufmann), vol. 10C, part 1, p. 120.

Hemsworth, R. S. 1986 Internal note JET-DN-C(86)24.

Jäckel, H., Magyar, G., Muller, R., Weller, A. & Zasche, D. 1986 In *Proc. 13th European Conference on Controlled Fusion and Plasma Heating, Schliersee, 14–18 April 1986* (ed. G. Briffod & M. Kaufmann), vol. 10C, part 1, p. 180.

Kaye, S. M. 1985 *Phys. Fluids* **28** (8), 2327.

Kaye, S. M. & Goldston, R. 1985 *Nucl. Fus.* **25**, 65.

Niedermeyer, H. *et al.* 1985 In *Proc. 12th European Conference on Controlled Fusion and Plasma Physics, Budapest, 2–6 September 1985* (*Europhysics conference abstracts* **9F** (1), 159).

Obert, W., Duesing, G., Küssel, E., Kupschus, P., Mayaux, C., Rebut, P. H. & Santos, H. 1984 In *Proc. 13th Symposium Fusion Technology, Varese*, p. 311.

Sadler, G., van Belle, P., Hone, M., Jarvis, O. N., Kallne, J. & Merlo, V. 1986 In *Proc. 13th European Conference on Controlled Fusion and Plasma Heating, Schliersee, 14–18 April 1986* (ed. G. Briffod & M. Kaufmann), vol. 10C, part 1, p. 105.

Sweetman, D. R., Cordey, J. G. & Green, T. S. 1981 *Phil. Trans. R. Soc. Lond.* A **300**, 689.

Watkins, M. & Stubberfield, P. M. 1986 In *Proc. 13th European Conference on Controlled Fusion and Plasma Heating, Schliersee, 14–18 April 1986* (ed. G. Briffod & M. Kaufmann), vol. 10C, part 1, p. 156.

PHILOSOPHICAL TRANSACTIONS OF THE ROYAL SOCIETY A MATHEMATICAL, PHYSICAL & ENGINEERING SCIENCES